



# Long-term fluxes of carbonyl sulfide and their seasonality and interannual variability in a boreal forest

5 Timo Vesala<sup>1,2,3</sup>, Kukka-Maaria Kohonen<sup>1</sup>, Arnaud P. Praplan<sup>4</sup>, Linda M.J. Kooijmans<sup>5</sup>, Lenka Foltýnová<sup>6</sup>, Pasi Kolari<sup>1</sup>, Markku Kulmala<sup>1</sup>, Jaana Bäck<sup>2</sup>, David Nelson<sup>7</sup>, Dan Yakir<sup>8</sup>, Mark Zahniser<sup>7</sup>,  
Ivan Mammarella<sup>1</sup>

<sup>1</sup>Institute for Atmospheric and Earth System Research / Physics, University of Helsinki, Helsinki, Finland

<sup>2</sup>Institute for Atmospheric and Earth System Research / Forest Sciences, University of Helsinki, Helsinki, Finland

<sup>3</sup>Yugra State University, 628012, Khanty-Mansiysk, Russia

<sup>4</sup>Finnish Meteorological Institute, Helsinki, Finland

10 <sup>5</sup>Meteorology and Air Quality, Wageningen University & Research, Wageningen, The Netherlands

<sup>6</sup>Global Change Research Institute, Czech Academy of Sciences, Brno, Czech Republic

<sup>7</sup>Aerodyne Research Inc., Billerica, MA, USA

<sup>8</sup>Weizmann Institute of Science, Rehovot, Israel

*Correspondence to:* Kukka-Maaria Kohonen (kukka-maaria.kohonen@helsinki.fi)

15 **Abstract.** The seasonality and interannual variability of terrestrial carbonyl sulfide (COS) fluxes are poorly constrained. We present the first easy-to-use parameterization for net COS forest sink based on the longest eddy covariance record from a boreal pine forest, covering 32 months over 5 years. Fluxes from hourly to yearly scales are reported, with the aim of revealing controlling factors and the level of interannual variability. The parameterization is based on the photosynthetically active radiation, vapor pressure deficit, air temperature, and leaf area index. The spring recovery of the flux after the winter dormancy period was mostly governed by air temperature, and the onset of the uptake varied by 2 weeks. For the first time, we report a significant reduction of ecosystem-scale COS uptake under large water vapor pressure deficit in summer. The maximum monthly and weekly median COS uptake varied 26 and 20 % between years, respectively. The timing of the latter varied by 6 weeks. The fraction of the nocturnal uptake remained below 21 % of the total COS uptake. We observed the growing season (April–August) average net flux of COS totaling  $-58.0 \text{ gS ha}^{-1}$  with 37 % interannual variability. The long-  
25 term flux observations were scaled up to evergreen needleleaf forests (ENFs) in the whole boreal region by the Simple Biosphere Model Version 4 (SiB4). The observations were closely simulated by using SiB4 meteorological drivers and phenology. The total COS uptake by boreal ENF was in line with a missing COS sink at high latitudes pointed out in earlier studies.

## 1 Introduction

30 During the last decade, carbonyl sulfide (COS) has attracted attention among the scientific community investigating the carbon cycle. Although the actual contribution of the exchange rate of COS between the biosphere and atmosphere to the ecosystem carbon balance is extremely small, COS has been proposed to provide a new insight into carbon dioxide (CO<sub>2</sub>)



exchange as a promising tracer (proxy) for the gross carbon uptake of plants (e.g., Stimler et al., 2010; Wohlfahrt et al., 2012; Asaf et al., 2013; Billesbach et al., 2014; Maseyk et al., 2014; Commane et al., 2015; Sun et al., 2016; Gimeno et al., 2017; Sun et al., 2018). The COS exchange can also provide valuable insight into the dynamics and estimates of the stomatal conductance regulating plant gas exchange and evapotranspiration (Wehr et al., 2017; Kooijmans et al., 2019; Stoy et al., 2019). Leaves and soil are the largest sink for COS (e.g., Kesselmeier et al., 1999; Whelan et al., 2018) and the net biosphere–atmosphere exchange of this trace gas has potential impact on the climate (e.g., Crutzen, 1976). COS affects climate through ozone chemistry and aerosol production besides its direct warming effect. Brühl et al. (2012) found that the consequent net cooling from aerosols is cancelled out by the warming.

The terrestrial plant COS uptake estimate has a broad range from 400 to 1360 Gg S y<sup>-1</sup> (Campbell et al., 2017). Recently the inversion modeling study by Ma et al. (2021) pointed to missing sources in the tropics and missing sinks at high latitudes. The factors controlling the COS flux (FCOS) temporal variability are partly unknown, although the dependence on temperature and light are rather well understood during the growing season (Commane et al., 2015; Wehr et al., 2017; Kooijmans et al., 2019). The prerequisite for fundamental understanding of the dynamics of the COS budget is *in situ* net ecosystem-scale flux observations with high time resolution by the eddy covariance (EC) method. Nevertheless, these direct flux measurements are still scarce. We report here the multiyear COS surface net flux for 32 months over 5 years from a boreal forest. This provides not only the opportunity to analyze the seasonality and interannual variability of the flux but also to create a representative parameterization presented here for the first time for the multiyear flux. The longest reported EC flux record before this study is from Wehr et al. (2017) from May through October for 2 years. They focused on average diurnal cycles and seasonality based on biweekly means in analyses of canopy stomatal conductance. The data presented here are unique in their location, being from the boreal region (mature Scots pine stand at Hyytiälä/SMEAR II station; Hari & Kulmala, 2005). The earlier reported EC records were collected from the Mediterranean (Asaf et al., 2013; Wohlfahrt et al., 2018; Yang et al., 2018; Spielmann et al., 2019) and temperate broadleaf ecosystems / arable land (Billesbach et al., 2014; Maseyk et al., 2014; Commane et al., 2015; Wehr et al., 2017; Spielmann et al., 2019).

Our objective is to report the net FCOSs and analyze them from hourly to yearly scales together with environmental conditions and other controlling factors, while paying attention to the seasonality and interannual variability. We hypothesize that the long-term FCOS can be described by a simple semi-empirical parameterization that employs radiation, air temperature ( $T_a$ ), humidity, and leaf area index (LAI). We test the hypothesis on our long time series. We analyze the dependence of FCOS on environmental factors both by using multivariate and univariate linear regressions, combining factors, and by applying wavelet analysis. COS balances with shares between day and nocturnal uptake are provided. We focus on the net ecosystem FCOS without partitioning into soil and canopy components since the net exchange is one of the main constraints on the atmospheric concentration, and especially because the multiyear dynamics of FCOS have not been previously studied. For canopy and soil COS exchange in the studied pine forest, see Kooijmans et al. (2017, 2019) and Sun



et al. (2018), respectively. Finally, we demonstrate the value of the long-term COS time series by using the upscaled parameterized FCOSs to evaluate FCOS simulations by the Simple Biosphere Model Version 4 (SiB4). We reflect on the results with the net CO<sub>2</sub> exchange but investigations of the gross carbon uptake are beyond the scope of this study.

## 70 2 Materials and methods

### 2.1 Site description

Measurements were made at the SMEAR II station, a boreal coniferous forest in Hyttiälä in southern Finland (61°51' N, 24°17' E, 181 m ASL) during the years 2013–2017. The site was dominated by Scots pine (*Pinus sylvestris* L.) with some Norway spruce (*Picea abies* (L.) Karst.) and deciduous trees (e.g., *Betula* sp., *Populus tremula*, *Sorbus aucuparia*) within at  
75 least a 150 m radius from the measurement mast. The tree density is ~1170 ha<sup>-1</sup> (Ilvesniemi et al. 2009), and the canopy height increased from approximately 18 m to 20 m during the measurement years. The Scots pine stand was established in 1962 (Hari & Kulmala, 2005). The long-term annual mean precipitation and the annual mean temperature are 711 mm and 3.5 °C, respectively (Pirinen et al. 2012).

### 2.2 Eddy covariance measurements and flux processing

80 EC measurements were made at 23 m height using an ultrasonic anemometer (Solent Research HS1199, Gill Instruments, Lymington, UK) to measure three wind components at 10 Hz frequency and an Aerodyne quantum cascade laser spectrometer (QCLS, Aerodyne Research, Billerica, MA, USA), which measured COS, CO<sub>2</sub>, water vapor (H<sub>2</sub>O), and since 2015 also carbon monoxide (CO) mole fractions also at 10 Hz. The gas flow rate was approximately 10 standard liters per minute. Background measurements of high-purity nitrogen were made every 30 min for 26 s to remove background spectral  
85 structures (Kooijmans et al., 2016). More detailed information about the measurement setup and flux calculation can be found in the Supplementary Information and Kohonen et al. (2020). The uncertainty of the cumulative FCOSs was estimated by the bootstrap method, assuming 20 % total uncertainty in FCOSs (Text S1, Kohonen et al., 2020) and taking the 95th percentile of the bootstrap. The FCOS record comprises 32 months over 5 years, of which 51 % is gap-filled, representing 23 152 measured 30 min fluxes, which provides the opportunity to observe and analyze the interannual variability.

### 90 2.3 Environmental variables and the commencement of the carbonyl sulfide uptake period

$T_a$  and relative humidity (RH) were measured at 16.8 and 33.6 m heights and an average of the two heights was assumed to best represent  $T_a$  and RH at 23 m height.  $T_a$  was measured by Pt100 sensors and RH calculated from the H<sub>2</sub>O mole fraction measured with a LI-COR LI-840 infrared light absorption analyzer and a Pt100 sensor. Photosynthetically active radiation (PAR) from 400 to 700 nm was measured above the canopy by a LI-COR LI-190SZ quantum sensor. Soil temperature ( $T_s$ ) in  
95 the A horizon (2–5 cm in the mineral soil) was determined as the mean of five locations, with data measured using Philips



KTY81-110 temperature sensors. Volumetric soil water content (SWC) in the A horizon (2–6 cm depth) was also calculated as the mean of five different locations, with data measured using a Campbell TDR100 time-domain reflectometer. For the calculation of the vapor pressure deficit (VPD), see Text S2.

100 Although the progress of COS uptake in the spring is a gradual process, we get a better insight into its evolution and its yearly variations if we define a threshold for the onset of COS uptake. For the commencement of the significant COS uptake period, we used the date when the midday FCOS permanently (for at least 5 consecutive days) fell below 30 % of the median of the minimum FCOS from all years (maximum uptake) (see Table S1). Daytime was defined as periods when the solar elevation angle was greater than zero.

#### 105 **2.4 Parameterization of carbonyl sulfide fluxes**

Parameters  $a = -341.81$ ,  $b = 1000$ ,  $c = -0.77$ , and  $d = 1.03$  were optimized using MATLAB's `fminsearch` function to find the smallest root mean square error of the parameterized FCOS against the measured FCOS. Parameter  $e = 0.18$  was fixed before optimizing the other parameters.

#### **2.5 Boreal region carbonyl sulfide fluxes**

110 We scaled up the FCOS parameterization to the whole boreal region to evaluate FCOS simulations by SiB4. SiB4 (Haynes et al., 2019) is a continuation of the SiB3 model in which COS exchange was implemented by Berry et al. (2013). One of the added capabilities of SiB4 that was not present in SiB3 is that it simulates fluxes of multiple plant functional types (PFTs) in a grid cell and allows selection of fluxes from a single PFT. This is beneficial for the analysis in this study where we want to compare with observation-based data from evergreen needleleaf forests (ENFs).

115

The COS module of SiB4 was recently updated with the COS soil exchange model of Ogee et al. (2016) and the standard COS mole fraction of 500 ppt was replaced by COS mole fraction fields that vary in space and time, including seasonal and diurnal variability (Kooijmans et al., 2021). The meteorological data that drive SiB4 are from the Modern-Era Retrospective analysis for Research and Applications (MERRA), available from 1980 onward (Gelaro et al., 2017). The simulations of  
120 SiB4 are preceded by a spin-up from 1850 to 1979 to initialize the carbon pools using the climatological average of available MERRA data (Smith et al., 2020). We ran SiB4 with 3-hourly output globally and for the analysis we selected grid cells (at  $0.5^\circ \times 0.5^\circ$  resolution) where ENFs cover more than 30 % of the land area in the northern hemisphere. The information on areal coverage of different PFTs was retrieved from MODIS data (Lawrence & Chase, 2007). Finally, only the fluxes representing ENF were selected.

125

To obtain COS biosphere fluxes for the whole boreal region based on the FCOS observations in Hyytiälä we repeated the FCOS parameterization with PAR, LAI (calculated in SiB4 from canopy carbon pools), canopy temperature, and VPD data

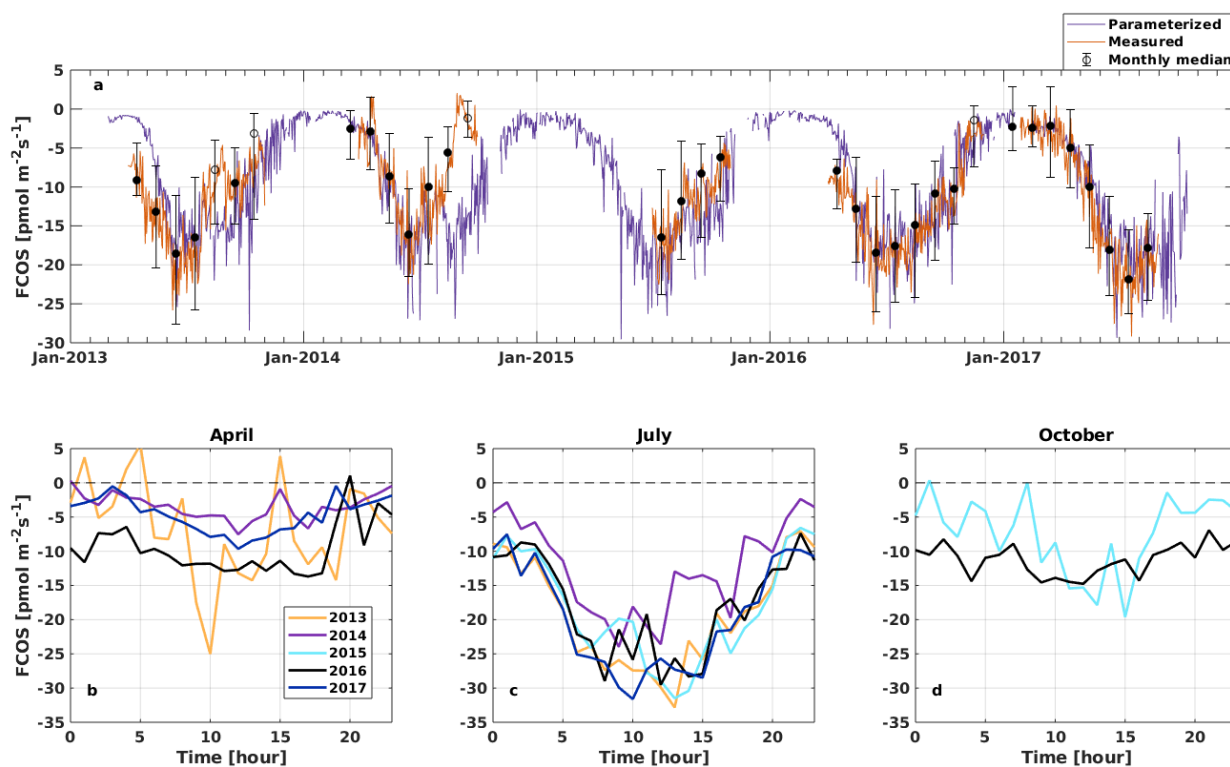


from SiB4 specifically for the grid cell where Hyytiälä is located. This yielded values of  $a = -77.7$ ,  $b = 1132.1$ ,  $c = -0.095$ ,  $d = 1$ , and  $e = 0.378$  for Eqs 2–5, where  $e$  is the original  $e$  multiplied by 2.1, the average ratio of Hyytiälä and SiB4 LAI data.  
130 We then applied this parameterization to the whole boreal region (based on the ENF grid cell selection described in the previous paragraph) using the SiB4 meteorological and phenological data.

### 3 Results and discussion

#### 3.1 Seasonality and its interannual variability

FCOS (COS uptake indicated by a negative sign) showed a pronounced seasonal cycle (Fig. 1a–d, Fig. S1) with the most  
135 negative flux in summer (June–August), which was expected as PAR,  $T_a$  and  $T_s$  also had clear seasonal cycles (Figs S2a and b, Fig. S3a).



140 **Figure 1.** Daily average net carbonyl sulfide flux (FCOS) time series (a) and median diurnal variation of FCOS in April (b), July (c), and October (d). A negative sign means COS uptake. Measured data (orange line in (a)) show daily gap-filled averages (see Text S1) and black circles represent the monthly medians. Filled circles mean that more than 20 % of data was measured, whereas empty circles indicate less than 20 % of measured data for that month. Whiskers show the 25th and 75th percentiles. The purple line in (a) is the parameterized daily FCOS (see Eq. 1). Plots b–d represent measured (non-gap-filled) data only. No data are available for 2015 in April and for 2013, 2014, and 2017 in October. Parameterized values are shown for 5 full years.



In April, years 2013 and 2016 represented higher uptake than years 2014 and 2017 (Fig. 1b). The significant COS uptake  
145 started on 15 April in 2013, based on a 3-day midday flux moving average being persistently below 30 % of the summer  
minimum (ca.  $-10 \text{ pmol m}^{-2} \text{ s}^{-1}$ ) (Table S1), and before 1 April (before measurements started) in 2016. The corresponding  
date was 28 April both in 2014 and 2017. Suni et al. (2003a) and Sevanto et al. (2006) studied the same forest stand as here  
and found that the spring recovery of the  $\text{CO}_2$  exchange is controlled by  $T_a$  to a large extent, whereas the soil water  
availability is not a limiting factor. However, the snow melt has been used as a good proxy indicator for the start of the  
150 carbon uptake (Pulliainen et al., 2017) in the boreal region. Suni et al. (2003a) defined the photosynthetically active period as  
when the  $\text{CO}_2$  flux reached 20 % of the maximum summer  $\text{CO}_2$  flux. They found that the days on which the daily average or  
a moving average  $T_a$  with a 5-day window exceeded 4.0 or 3.3 °C, respectively, coincided accurately with the  
commencement day of the photosynthetically active period. We analyzed the dependence of  $\text{CO}_2$  flux on  $T_a$  for the period of  
this study and no similar corresponding relationship was found for  $\text{CO}_2$  nor for FCOS. When the median  $T_a$  of May in 2014  
155 and 2017 was low (below 8 °C), the FCOS remained above  $-9 \text{ pmol m}^{-2} \text{ s}^{-1}$ , whereas it was ca.  $-13 \text{ pmol m}^{-2} \text{ s}^{-1}$  in 2013  
and 2016 when the median  $T_a$  was ca. 13 °C (Table S2, Fig. S4). During spring (April–May) the higher VPD was positively  
correlated with the COS uptake, but this resulted from higher  $T_a$ , which was also positively correlated (see Figs 2b and c).  
The heat sum (sum of daily average temperatures that are above 0 °C) did not influence the commencement of significant  
COS uptake in the spring (Fig. S5).

160

The COS uptake in July 2014 was at a significantly lower level in the afternoon than in other years (Fig. 1c).  $T_a$  and VPD  
having maximum values in the afternoon were larger in July 2014 than in any other year (Fig. S4). This led to the most  
pronounced asymmetry in the uptake between the morning and afternoon in July 2014. The monthly median COS uptake  
was 54 % smaller in July 2014 compared with that in 2017 when the uptake was the largest (Table S2). The forest acted as a  
165 COS sink during nighttime throughout the measurement period (see Fig. 4). Previous measurements have found both  
nocturnal soil uptake (Sun et al., 2018), but also uptake by foliage, as suggested by the stomatal conductance being non-zero  
throughout the night, indicating incomplete stomatal closure during nighttime (Kooijmans et al., 2017; 2019). The average  
nocturnal FCOS varied between  $-5$  to  $-12 \text{ pmol m}^{-2} \text{ s}^{-1}$  throughout the year. Compared with July, the diurnal variation in  
FCOS was much smaller in April and October, especially in 2016 (Figs 1b–d). The flux was close to zero but still indicated  
170 small uptake during winter months when data were available in November 2016–March 2017 (monthly median between  
 $-2.4$  and  $-1.5 \text{ pmol m}^{-2} \text{ s}^{-1}$ ) (Fig. 1a, Table S2). Suni et al. (2003b) found that light is the determining factor for the cessation  
of the growing season for the same stand. For the parameterized flux in Fig. 1a, see Sect. 3.3.

The lowest monthly median FCOS (highest uptake) was  $-21.9 \text{ pmol m}^{-2} \text{ s}^{-1}$  in July 2017 (Table S2). In June 2014 the  
175 monthly FCOS was  $-16.1 \text{ pmol m}^{-2} \text{ s}^{-1}$ , which is the highest flux from the months of the biggest uptake in each year. The  
lowest weekly FCOS was  $-23.9 \text{ pmol m}^{-2} \text{ s}^{-1}$  in week 29 (20–26 July) in 2017, and the highest was  $-19.2 \text{ pmol m}^{-2} \text{ s}^{-1}$  in  
week 25 in 2014 (16–22 July), from the weeks of the biggest uptake in each year. Thus, the interannual variability in the



maximum uptake is 26 and 20 % in the monthly and weekly medians, respectively. The variability in the timing of the maximum weekly uptake was 6 weeks, occurring in week 23 in 2016 and week 29 in 2017 (Table S3).

### 180 3.2 Carbonyl sulfide flux relationship on light, air temperature, and vapor pressure deficit

Fig. 2 presents FCOS as a function of PAR,  $T_a$ , and VPD for April–May and June–August. For the other responses and unfiltered data, see Fig. S6. The fluxes showed a clear relationship with PAR (Figs 2a and d), even though the COS biochemical reactions are light independent and FCOS responds to light only due to the light response of stomatal conductance (Kooijmans et al., 2019). When  $T_a$  was high (Fig. 2e), in theory favoring the uptake due to enhanced  
185 biochemical reactions in the mesophyll, the simultaneous occurrence of high VPD (Fig. 2f) limited the uptake due to smaller stomatal conductance values (see Kooijmans et al., 2019). The fluxes tended to saturate as a function of  $T_a$  above 10 °C in spring and increase (uptake decrease) above 15 °C in summer (Figs 2b and e, respectively). At 10 °C in spring FCOS was ca. -15  $\mu\text{mol m}^{-2} \text{s}^{-1}$ , whereas in summer ca. -25  $\mu\text{mol m}^{-2} \text{s}^{-1}$ . These flux values correspond to VPD of ca. 1 kPa in spring and summer, respectively. The non-zero value in the dark represents the ecosystem nocturnal COS uptake (Fig. 2a). The  
190 response curve saturated at high PAR values in the summer to approximately twice the level of those in spring. The saturation occurred above the PAR value of about 500  $\mu\text{mol m}^{-2} \text{s}^{-1}$ . Correspondence with VPD resembled that on  $T_a$  (Figs 2c and f). The fluxes tended to increase (uptake decrease) when VPD was above 0.8 kPa.

We analyzed the relationship between FCOS and environmental factors using multivariate and univariate linear regressions  
195 (Text S3) combining VPD, relative humidity (RH), net radiation ( $R_n$ ) or PAR,  $T_a$  or  $T_s$ , SWC, and precipitation. Their intercorrelation was of an acceptable level for the analysis (Text S3). Daily FCOS was best explained by VPD,  $R_n$ ,  $T_s$ , and SWC ( $R^2 = 0.65$ , Table 1), where the contribution of SWC was minor (see also Kooijmans et al., 2019). Primary variables directly interacting with the canopy (VPD, PAR, and  $T_a$ ) explained FCOS with  $R^2 = 0.53$ . On a monthly scale, replacing VPD by precipitation gave the highest  $R^2$  (0.88), while  $R^2$  (VPD, PAR,  $T_a$ ) = 0.77. Univariate analysis for single factors  
200 revealed that the temperature was the most important factor governing FCOS (Table 1).

We also applied wavelet analysis (Text S4; Torrence & Gilbert, 1998). It revealed coherence between FCOS and PAR on daily and yearly temporal scales without any significant time lags between them (Fig. S7), indicating a rapid response of stomata to PAR. The pattern of the coherence between FCOS and VPD was very similar, although the coherence values  
205 were somewhat smaller than those with PAR. The coherence between  $T_a$  and FCOS had a 3-hour lag on a daily scale, so minimum FCOS (uptake maximum) was reached before the  $T_a$  maximum.  $T_a$  reached its daily maximum usually in the afternoon between 3:00 and 5:00 pm (not shown), while FCOS minima were most frequently between 10:00 am and 2:00 pm (Fig. 1c). This is caused by VPD and PAR, which control the stomatal conductance (Fig. S7, Kooijmans et al., 2019). On a yearly scale there was no significant phase difference between  $T_a$  and FCOS.

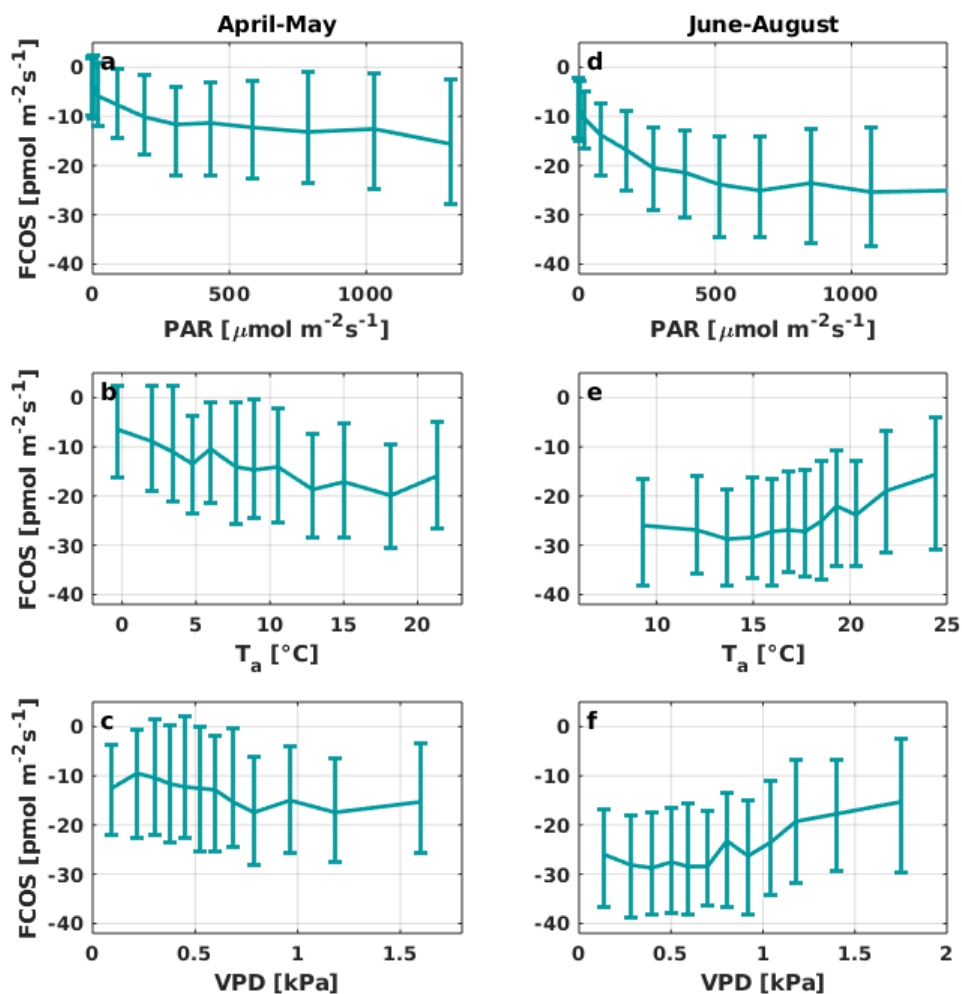


Figure 2. Carbonyl sulfide flux (FCOS) relationship with environmental variables in spring (a–c) and summer (d–f). Plots b, c, e, and f are filtered to high radiation only (photosynthetically active radiation,  $\text{PAR} > 500 \mu\text{mol m}^{-2} \text{s}^{-1}$ ). Data are binned in 12 equally sized bins and whiskers represent the 25th and 75th percentiles. VPD = vapor pressure deficit.





215

		Daily		Weekly		Monthly	
		R <sup>2</sup>	P	R <sup>2</sup>	P	R <sup>2</sup>	P
Multivariate regressions	VPD + T <sub>s</sub> + R <sub>n</sub> + SWC	0.65	<0.001	0.86	<0.001	—	—
	VPD + T <sub>a</sub> + R <sub>n</sub> + SWC	0.61	<0.001	0.80	<0.001	—	—
	VPD + PAR + SWC + T <sub>s</sub>	0.60	<0.001	0.82	<0.001	—	—
	VPD + T <sub>a</sub> + R <sub>n</sub>	0.58	<0.001	0.76	<0.001	—	—
	VPD + PAR + T <sub>s</sub>	0.55	<0.001	0.79	<0.001	—	—
	VPD + T <sub>a</sub> + PAR + SWC	0.54	<0.001	0.73	<0.001	—	—
	VPD + T <sub>a</sub> + PAR	0.53	<0.001	0.73	<0.001	0.77	<0.001
	Precip + T <sub>s</sub> + SWC + R <sub>n</sub>	—	—	—	—	0.88	<0.001
	Precip + T <sub>s</sub> + SWC + PAR	—	—	—	—	0.86	<0.001
	Precip + T <sub>s</sub> + SWC	—	—	—	—	0.85	<0.001
	Precip + T <sub>a</sub> + SWC	—	—	—	—	0.82	<0.001
Univariate regressions	T <sub>s</sub>	0.46	<0.001	0.68	<0.001	0.71	<0.001
	T <sub>a</sub>	0.39	<0.001	0.63	<0.001	0.70	<0.001
	R <sub>n</sub>	0.27	<0.001	0.42	<0.001	0.28	0.04
	PAR	0.13	<0.001	0.28	<0.001	0.24	0.03
	χ <sub>cos</sub>	0.13	<0.001	0.19	<0.001	0.24	0.03
	VPD	0.04	<0.001	0.15	<0.001	0.17	0.08
	SWC	0.04	<0.001	0.06	0.03	0.02	0.51
	RH	0.00	0.43	0.00	0.98	0.02	0.54
	Precip	0.00	0.24	0.12	0.002	0.49	<0.00

**Table 1.** Results of the multivariate and univariate regression analysis for carbonyl sulfide (COS) flux at daily, weekly, and monthly timescales. Variables tested are vapor pressure deficit (VPD), air temperature (T<sub>a</sub>), photosynthetically active radiation (PAR), net radiation (R<sub>n</sub>), soil water content (SWC), soil temperature (T<sub>s</sub>), precipitation (Precip), relative humidity (RH), and atmospheric COS mixing ratio (χ<sub>cos</sub>). Two variables related to the similar physical quantity were never used in the same model (T<sub>a</sub> and T<sub>s</sub>, PAR and R<sub>n</sub>, or RH and VPD). All the models which included more than one variable were tested with the variation inflation factor, which was in all cases less than 5, showing that intercorrelation of the variables is negligible.

220

### 3.3 Parameterization of the net carbonyl sulfide flux

FCOS was parameterized using PAR, T<sub>a</sub>, VPD, and total LAI data over the 32 months on a daily scale. Since the ecosystem COS uptake is dominated by the canopy uptake (70% at minimum according to Sun et al., 2018) and is process-wise very close to the CO<sub>2</sub> uptake, we formulated the parameterization as follows:

225

$$FCOS = FPAR * FS * FVPD * FLAI \quad (1)$$



where

230

$$F_{PAR} = \frac{a * PAR}{PAR + b} \quad (2)$$

$$FS = \frac{1}{1 + \exp(c * S)} \quad (3)$$

$$F_{VPD} = \frac{d}{1 + \sqrt{VPD}} \quad (4)$$

$$FLAI = \frac{1 - \exp(-e * LAI)}{e} \quad (5)$$

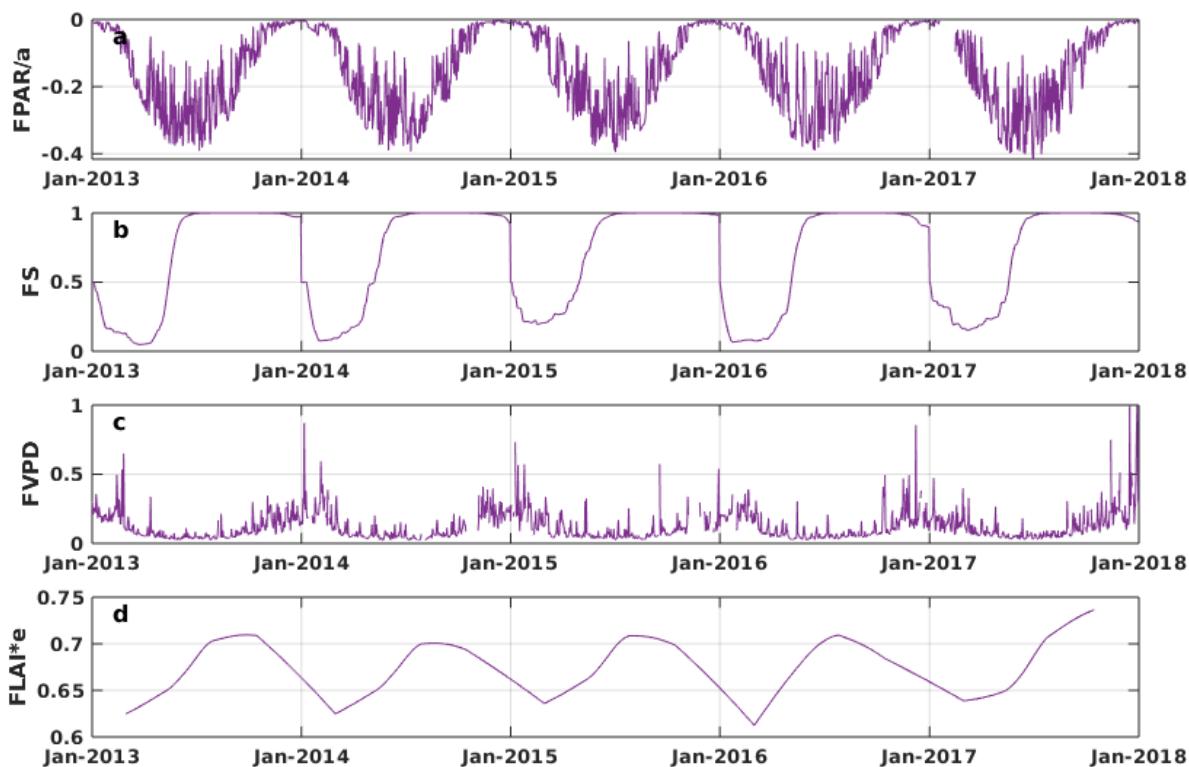
235

where  $a$ ,  $b$ ,  $c$ ,  $d$ , and  $e$  are fitting parameters and four functions are simplified from the corresponding dependencies of the  $\text{CO}_2$  uptake on PAR and  $T_a$  ( $S$  being a function of  $T_a$ ; see Text S2) (according to Mäkelä et al., 2008), VPD (Dewar et al., 2018), and LAI (Peltoniemi et al., 2015). Although recognizing that other more complex formulas with more fitting parameters could provide better correspondence with observations, we desired to keep the parameterization simple for the sake of generic process description: here  $F_{PAR}$  describes the stomatal response to PAR,  $FS$  the phenology of biochemical reactions,  $F_{VPD}$  the stomatal regulation, and  $FLAI$  the amount of foliage and canopy light penetration. Parameter values of  $a = -341.81$ ,  $b = 1000$ ,  $c = -0.77$ ,  $d = 1.03$ , and  $e = 0.18$  gave the best optimization against the measured FCOS (Fig. 1a). Fig. 3 presents the modulation of the four variables of the FCOS, where  $FS$  has the biggest effect via  $T_a$  governing seasonality and LAI the smallest one. At the same time, PAR varied between 0 and 1870  $\mu\text{mol m}^{-2} \text{s}^{-1}$ ,  $T_a$  between  $-28$  and  $+29$  °C, VPD between 0 and 2.7 kPa, and LAI between 5.3 and 7.4  $\text{m}^2 \text{m}^{-2}$ . Eq. 1 provides a robust description of the average FCOS dynamics from a yearly to daily scale ( $R^2 = 0.57$ ) (Fig. 1a and Figs S8 and S9, respectively). The difference of the parameterization to the gap-filling function presented in Kohonen et al., (2020) and Text S1, is that unlike the gap-filling function, this simple parameterization does not require evaluation of parameter values against measurements every two weeks. The evolution of FCOS is taken into account solely with environmental variables. The prediction from Eq. 1 differs from the monthly medians, with at least 20 % of data measured (filled circles in Fig. 1a), mostly in April-June 2013, July-August 2014 and September 2015. In 2016–2017, the predicted values closely follow the measured data excluding April 2016.

240

245

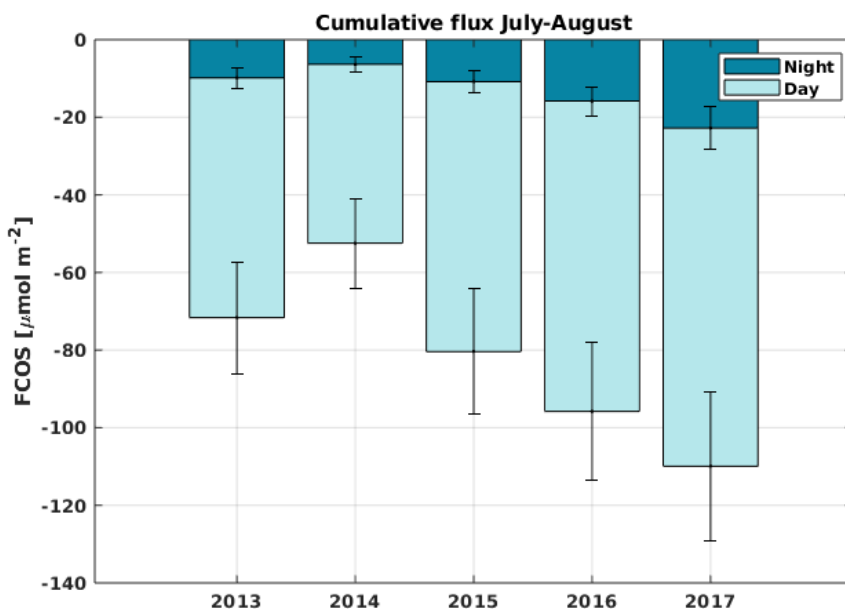
250



255 **Figure 3.** Time series of the daily average values of the parameter functions (Eqs 2–5) normalized to vary between 0 and 1. FLAI = foliage and canopy light penetration, FPAR = stomatal response to PAR, FS = phenology of biochemical reactions, FVPD = stomatal regulation.

### 3.4 Carbonyl sulfide balances and their interannual variation

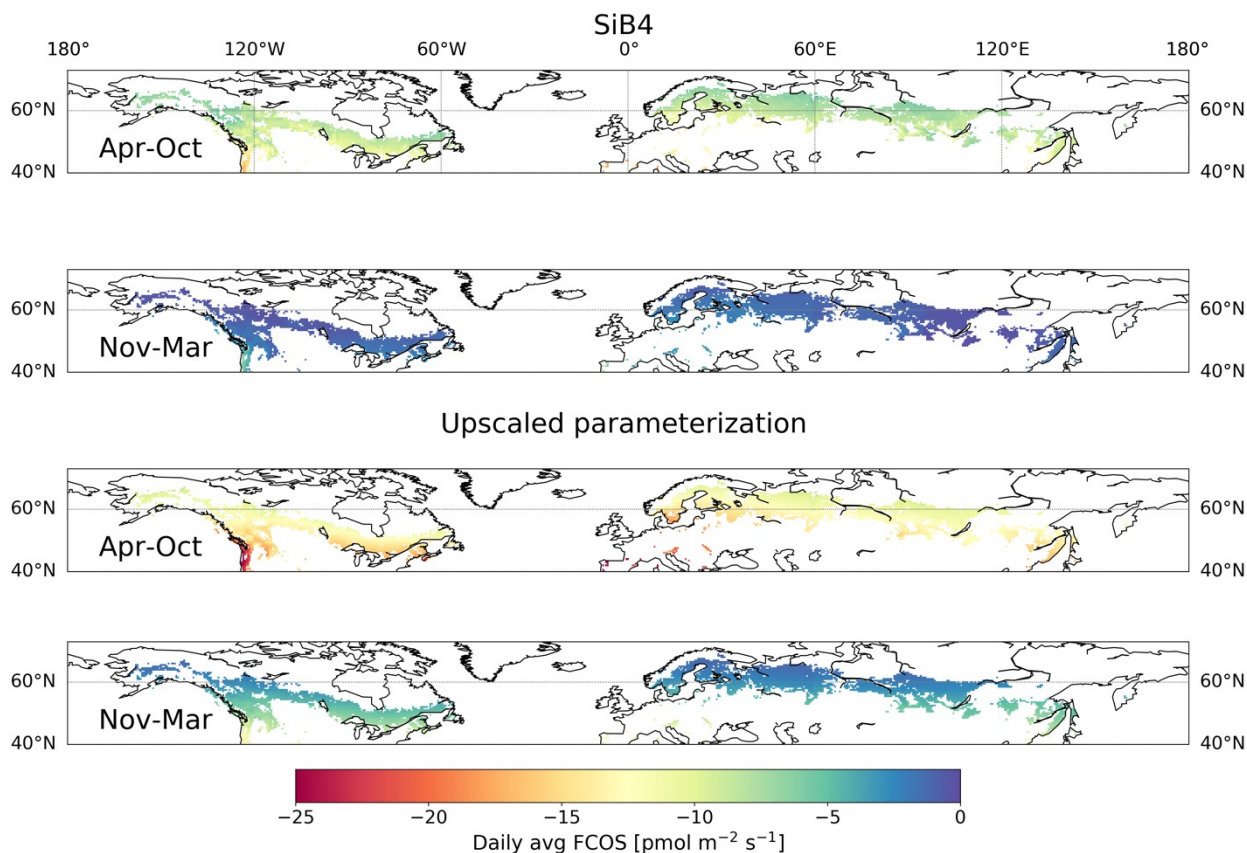
We analyzed COS balances, the share between day- and nighttime uptake, and their interannual variability. The cumulative FCOS (FCOS<sub>cum</sub>) values are presented in Fig. 4 for the periods of the smallest amount of gap-filled data, that is, July–August  
260 in 2013–2017. FCOS<sub>cum</sub> in 2014 was 52 % lower than in 2017. The larger total uptakes were not only due to daytime uptake. The higher absolute nighttime uptake corresponded not only to the higher total uptake but also to the higher nocturnal percentage of the total uptake. The cumulative nocturnal uptake fraction of the total uptake was 0.14, 0.12, 0.15, 0.17, and 0.21 for years 2013–2017, respectively. The total FCOS<sub>cum</sub> for the period April–August was  $-183 \pm 41$  ( $-58.5 \pm 13$ ),  
265  $-130 \pm 30$  ( $-41.6 \pm 9.6$ ),  $-207 \pm 45$  ( $-66.4 \pm 14.4$ ),  $-205 \pm 45$  ( $-65.5 \pm 14.4$ )  $\mu\text{mol COS m}^{-2}$  (or  $\text{gS ha}^{-1}$ ) for years 2013, 2014, 2016, and 2017, respectively. The annual sulfur deposition of sulfate and sulfur dioxide (SO<sub>2</sub>) is estimated to be 780  $\text{gS ha}^{-1}$  (pers. comm. Hannele Hakola, Finnish Meteorological Institute) for the measurement site. The COS sulfur deposition reported here was thus 7 % of that of sulfate and SO<sub>2</sub>.



270 **Figure 4.** Cumulative sum of gap-filled carbonyl sulfide flux (FCOS) in 2013–2017 during the period July–August, separated into day and night contributions. The percentage of gap-filled COS data during nighttime and daytime, respectively, was 77 and 58 % in 2013, 70 and 45 % in 2014, 57 and 38 % in 2015, 65 and 43 % in 2016, and 55 and 29 % in 2017.

### 3.5 Implications for global biogeochemical cycles

The long-term time series presented in this study, together with the relationships of the FCOS with PAR,  $T_a$ , VPD, and LAI, can help to evaluate and improve biosphere models and thereby contribute to an accurate biosphere sink estimate. We scaled  
275 up the FCOS parameterization to the whole boreal region to evaluate FCOS simulations by SiB4. To do this, we repeated the FCOS parameterization with the meteorological and phenological data that are used and simulated by SiB4 for the grid cell where Hyytiälä is located. We then applied this parameterization to the whole boreal region using the SiB4 meteorological and phenological data. The resulting daytime average FCOS in the boreal region is always larger than the FCOS simulated by SiB4, especially in the summer months (Fig. 5, see Fig. S10 for the difference between the two methods). The total FCOS  
280 of evergreen needleleaf forests (ENFs) in the boreal region is estimated to be  $-16.6 \text{ Gg S y}^{-1}$  by the parameterization for the years 2013–2017, 1.6 times larger than that simulated by SiB4 ( $-10.6 \text{ Gg S y}^{-1}$ ). These results are in line with the inverse modeling study by Ma et al. (2021), who pointed to a missing sink in the higher latitudes of the northern hemisphere. The parameterization presented here could serve to improve the prior descriptions of the COS biosphere flux used for inverse modeling studies like that of Ma et al. (2021). Such an approach would provide more accurate COS biosphere sink estimates  
285 and could help to improve the representation of gross primary production in biosphere models as well.



290 **Figure 5.** Daily average (avg) carbonyl sulfide flux (FCOS) in the boreal region based on SiB4 (top) and upscaled parameterization simulations (bottom) for the periods April–October and November–March. The boreal region is defined as the area where evergreen needleleaf forests cover more than 30 % of the land area in the northern hemisphere.

#### 4 Conclusions

In summary, to get a more accurate picture of temporal dynamics and variations of the FCOS between the atmosphere and biosphere, multiyear observations are needed. Here a clear relationship between the spring recovery and the FCOS and temperature thresholds or sums was not observed. The significant reduction of the FCOS under large VPD values on the ecosystem scale found here corroborates the relationship observed between the shoot-scale FCOS and VPD at the same forest by Kooijmans et al. (2019), who illustrated the stomatal limitation of the flux. The contribution of COS to the total annual sulfur deposition was estimated to be 7 %. We hypothesized that the long-term FCOS can be described by a simple semi-empirical parameterization that employs PAR,  $T_a$ , VPD, and LAI. We tested the hypothesis with our long time series. We proved the hypothesis by presenting the first easy-to-use parameterization for the FCOS. We scaled up the FCOS parameterization to the whole boreal region and the obtained results are in line with the inverse modeling study by Ma et al. (2021), who pointed to a missing sink in the higher latitudes of the northern hemisphere. It remains to be studied whether

295  
300



305 multiyear dynamics and seasonal patterns in the in situ flux analyzed here are reflected also in regional terrestrial COS air concentration and sink observations and estimates.

### Acknowledgments

310 Special thanks to Helmi Keskinen, Sirpa Rantanen, Janne Levula, and other Hyttiälä technical staff for all their support with the measurements. The authors thank the Academy of Finland Centre of Excellence (118780), Academy Professor projects (312571 and 282842), ICOS Finland (3119871), ACCC Flagship funded by the Academy of Finland grant number 337549 and the Tyumen region government in accordance with the Program of the World-Class West Siberian Interregional Scientific and Educational Center (National Project “Nauka”). K.-M. Kohonen thanks the Vilho, Yrjö and Kalle Väisälä foundation for its support. L.M.J. Kooijmans thanks the ERC advanced funding scheme (COS-OCS, 742798).

### Author contributions

315 TV, IM and KMK designed the study. KMK, PK and AP performed the measurements and flux processing. MZ and DN helped with the flux measurements and setup. KMK, LMJK and LF performed the data analysis: KMK developed the local flux parameterization and LMJK expanded the parameterization for the boreal region, while LF did the multivariate analysis. MK, JB and DY commented the manuscript. TV and KMK wrote the manuscript with contributions from all co-authors.

### Competing interests

The authors declare that they have no conflict of interest.

### 320 Data availability

Environmental data used in the study are available in the AVAA – Open research data publishing platform (<https://smear.avaa.csc.fi/>). The metadata of the observations are available via the Etsin service. Flux data will be published in a public repository before publication.

### References

325 Asaf, D., Rotenberg, E., Tatarinov, F., Dicken, U., Montzka, S. A., & Yakir, D. (2013). Ecosystem photosynthesis inferred from measurements of carbonyl sulphide flux. *Nature Geoscience*, 6(3), 186.

Berry, J., Wolf, A., Campbell, J. E., Baker, I., Blake, N., Blake, D., Denning, A. S., Kawa, S. R., Montzka, S. A., Seibt, U., Stimler, K., Yakir, D. & Zhu, Z. (2013). A coupled model of the global cycles of carbonyl sulfide and CO<sub>2</sub>: A possible new window on the carbon cycle. *Journal of Geophysical Research: Biogeosciences*, 118(2), 842-852.



- 330 Billesbach, D. P., Berry, J. A., Seibt, U., Maseyk, K., Torn, M. S., Fischer, M. L., Abu-Naser, M. & Campbell, J. E. (2014). Growing season eddy covariance measurements of carbonyl sulfide and CO<sub>2</sub> fluxes: COS and CO<sub>2</sub> relationships in Southern Great Plains winter wheat. *Agricultural and forest meteorology*, 184, 48-55.
- Brühl, C., Lelieveld, J., Crutzen, P. J., & Tost, H. (2012). The role of carbonyl sulphide as a source of stratospheric sulphate aerosol and its impact on climate. *Atmospheric Chemistry and Physics*, 12(3), 1239-1253.
- 335 Campbell, J. E., Berry, J. A., Seibt, U., Smith, S. J., Montzka, S. A., Launois, T., ... & Laine, M. (2017). Large historical growth in global terrestrial gross primary production. *Nature*, 544(7648), 84-87.
- Commane, R., Meredith, L. K., Baker, I. T., Berry, J. A., Munger, J. W., Montzka, S. A., Templer, P. H., Juice, S. M., Zahniser, M. S. & Wofsy, S. C. (2015). Seasonal fluxes of carbonyl sulfide in a midlatitude forest. *Proceedings of the National Academy of Sciences*, 112(46), 14162-14167.
- 340 Crutzen, P. J. (1976). The possible importance of CSO for the sulfate layer of the stratosphere. *Geophysical Research Letters*, 3(2), 73-76.
- Dewar, R., Mauranen, A., Mäkelä, A., Hölttä, T., Medlyn, B., & Vesala, T. (2018). New insights into the covariation of stomatal, mesophyll and hydraulic conductances from optimization models incorporating nonstomatal limitations to photosynthesis. *New Phytologist*, 217(2), 571-585.
- 345 Fox, J. and Weisberg, S. (2011). *An R Companion to Applied Regression*, Second Edition. Thousand Oaks CA: Sage. URL: <http://socserv.socsci.mcmaster.ca/jfox/Books/Companion>
- Gelaro R, McCarty W, Suarez MJ, Todling R, Molod A, Takacs L, et al. The modern-era retrospective analysis for research and applications, version 2 (MERRA-2). *Journal of Climate*. 2017;30(14):5419-5454.
- Gimeno, T. E., Ogée, J., Royles, J., Gibon, Y., West, J. B., Burlett, R., Jones, S. P., Sauze, J., Wohl, S., Benard, C., Genty, B. & Wingate, L. (2017). Bryophyte gas-exchange dynamics along varying hydration status reveal a significant carbonyl sulphide (COS) sink in the dark and COS source in the light. *New Phytologist*, 215(3), 965-976.
- 350 Grinsted, A., Moore, J. C., & Jevrejeva, S. (2004). Application of the cross wavelet transform and wavelet coherence to geophysical time series. *Nonlinear processes in geophysics*, 11(5/6), 561-566.
- Hari, P. & Kulmala, M. (2005). Station for Measuring Ecosystem–Atmosphere Relations (SMEAR II), *Boreal Environment Research* 10.5, 315–322



- Haynes, K.D., Baker, I.T., Denning, A.S., Stöckli, R., Schaefer, K., Lokupitiya, E.Y., & Haynes, J.M. (2019). Representing grasslands using dynamic prognostic phenology based on biological growth stages: 1. Implementation in the Simple Biosphere Model (SiB4). *Journal of Advances in Modeling Earth Systems*, 11, <https://doi.org/10.1029/2018MS001540>.
- 360 Kesselmeier, J., Teusch, N., & Kuhn, U. (1999). Controlling variables for the uptake of atmospheric carbonyl sulfide by soil. *Journal of Geophysical Research: Atmospheres*, 104(D9), 11577-11584.
- Kohonen, K.-M., Kolari, P., Kooijmans, L. M. J., Chen, H., Seibt, U., Sun, W., and Mammarella, I. (2020). Towards standardized processing of eddy covariance flux measurements of carbonyl sulfide, *Atmos. Meas. Tech.*, 13, 3957–3975.
- Kooijmans, L. M., Uitslag, N. A., Zahniser, M. S., Nelson, D. D., Montzka, S. A., & Chen, H. (2016). Continuous and high-precision atmospheric concentration measurements of COS, CO<sub>2</sub>, CO and H<sub>2</sub>O using a quantum cascade laser spectrometer (QCLS). *Atmospheric Measurement Techniques*, 9(11), 5293-5314.
- 365 Kooijmans, L. M., Maseyk, K., Seibt, U., Sun, W., Vesala, T., Mammarella, I., Kolari, P., Aalto, J., Franchin, A., Vecchi, R., Valli, G. & Chen, H. (2017). Canopy uptake dominates nighttime carbonyl sulfide fluxes in a boreal forest. *Atmospheric Chemistry and Physics*, 17(18), 11453-11465.
- Kooijmans, L. M., Sun, W., Aalto, J., Erkkilä, K. M., Maseyk, K., Seibt, U., Vesala, T., Mammarella, I. & Chen, H. (2019). Influences of light and humidity on carbonyl sulfide-based estimates of photosynthesis. *Proceedings of the National Academy of Sciences*, 116(7), 2470-2475.
- 370 Kooijmans, L. M. J., Cho, A., Ma, J., Kaushik, A., Haynes, K. D., Baker, I., Luijkx, I. T., Groenink, M., Peters, W., Miller, J. B., Berry, J. A., Ogée, J., Meredith, L. K., Sun, W., Kohonen, K.-M., Vesala, T., Mammarella, I., Chen, H., Spielmann, F. M., Wohlfahrt, G., Berkelhammer, M., Whelan, M. E., Maseyk, K., Seibt, U., Commane, R., Wehr, R., and Krol, M.: Evaluation of carbonyl sulfide biosphere exchange in the Simple Biosphere Model (SiB4), *Biogeosciences Discuss.* [preprint], <https://doi.org/10.5194/bg-2021-192>, in review, 2021.
- Lau, K.-M. and Weng, H. (1995). Climate signal detection using wavelet transform: How to make a time series sing. *Bulletin of the American Meteorological Society*, 76(12), 2391-2402.
- Lawrence, P.J. and T.N. Chase, 2007, Representing a new MODIS consistent land surface in the Community Land Model (CLM 3.0). *J. Geophys. Res.*, 112, G01023.
- 380 Ma, J., Kooijmans, L. M. J., Cho, A., Montzka, S. A., Glatthor, N., Worden, J. R., Kuai, L., Atlas, E. L., and Krol, M. C. (2021). Inverse modelling of carbonyl sulfide: implementation, evaluation and implications for the global budget, *Atmos. Chem. Phys.*, 21, 3507–3529, <https://doi.org/10.5194/acp-21-3507-2021>, 2021.





- 385 Mammarella, I., Launiainen, S., Grönholm, T., Keronen, P., Pumpanen, J., Rannik, Ü., & Vesala, T. (2009). Relative humidity effect on the high-frequency attenuation of water vapor flux measured by a closed-path eddy covariance system. *Journal of Atmospheric and Oceanic Technology*, 26(9), 1856-1866.
- Mammarella, I., Peltola, O., Nordbo, A., Järvi, L., and Rannik, Ü. (2016). Quantifying the uncertainty of eddy covariance fluxes due to the use of different software packages and combinations of processing steps in two contrasting ecosystems, *Atmos. Meas. Tech.*, 9, 4915-4933, <https://doi.org/10.5194/amt-9-4915-2016>
- 390 Maseyk, K., Berry, J. A., Billesbach, D., Campbell, J. E., Torn, M. S., Zahniser, M., & Seibt, U. (2014). Sources and sinks of carbonyl sulfide in an agricultural field in the Southern Great Plains. *Proceedings of the National Academy of Sciences*, 111(25), 9064-9069.
- Mäkelä, A., Pulkkinen, M., Kolari, P., Lagergren, F., Berbigier, P., Lindroth, A., Loustau, D., Nikinmaa, E., Vesala, T., and Hari, P. 2008. Developing an empirical model of stand GPP with the LUE approach: analysis of eddy covariance data at five  
395 contrasting conifer sites in Europe. *Global Change Biology*, 14, 92-108.
- Ogée, J., Sauze, J., Kesselmeier, J., Genty, B., Van Diest, H., Launois, T., & Wingate, L. (2016). A new mechanistic framework to predict OCS fluxes from soils. *Biogeosciences*, 13(8), 2221-2240.
- Pelkonen, P., & Hari, P. (1980). The dependence of the springtime recovery of CO<sub>2</sub> uptake in Scots pine on temperature and internal factors. *Flora*, 169(5), 398-404.
- 400 Peltoniemi, M., Pulkkinen M., Aurela M., Pumpanen J., Kolari P. & Mäkelä, A. 2015: a semi-empirical model of boreal-forest gross primary production, evapotranspiration, and soil water — calibration and sensitivity analysis. *Boreal Env. Res.* 20: 151–171
- Pulliainen, J., Aurela, M., Laurila, T., Aalto, T., Takala, M., Salminen, M., Kulmala, M., Barr, A., Heimann, M., Lindroth, A., Laaksonen, A., Derksen, C., Mäkelä, A., Markkanen, T., Lemmetyinen, J., Susiluoto, J., Dengel, S., Mammarella, I.,  
405 Tuovinen, J-P. and Vesala, T. (2017). Early snowmelt significantly enhances boreal springtime carbon uptake. *Proceedings of the National Academy of Sciences*, 114(42), 11081-11086.
- R Core Team (2019). R: A language and environment for statistical computing. R Foundation for Statistical Computing, Vienna, Austria. URL <https://www.R-project.org/>.
- Rannik, Ü., & Vesala, T. (1999). Autoregressive filtering versus linear detrending in estimation of fluxes by the eddy  
410 covariance method. *Boundary-Layer Meteorology*, 91(2), 259-280.
- Sevanto, S., Suni, T., Pumpanen, J., Grönholm, T., Kolari, P., Nikinmaa, E., Hari, P. & Vesala, T. (2006). Wintertime photosynthesis and water uptake in a boreal forest. *Tree Physiology*, 26(6), 749-757.



- Smith, N. E., Kooijmans, L. M., Koren, G., van Schaik, E., van der Woude, A. M., Wanders, N., Ramonet, M., Xueref-Remy, I., Siebicke, L., Manca, G., Brümmner, C., Baker, I. T., Haynes, K. D., Lujikx, I., & Peters, W. (2020). Spring  
415 enhancement and summer reduction in carbon uptake during the 2018 drought in northwestern Europe. *Philosophical Transactions of the Royal Society B*, 375(1810), 20190509, <http://dx.doi.org/10.1098/rstb.2019.0509>.
- Spielmann, F. M., Wohlfahrt, G., Hammerle, A., Kitz, F., Migliavacca, M., Alberti, G., Ibrom, A., El-Madany, T. S., Gerdel, K., Moreno, G., Kolle, O., Karl, T., Peressotti, A. & Delle Vedove, G.. (2019). Gross primary productivity of four European ecosystems constrained by joint CO<sub>2</sub> and COS flux measurements. *Geophysical Research Letters*, 46(10), 5284-5293.
- 420 Stimler, K., Montzka, S. A., Berry, J. A., Rudich, Y., & Yakir, D. (2010). Relationships between carbonyl sulfide (COS) and CO<sub>2</sub> during leaf gas exchange. *New Phytologist*, 186(4), 869-878.
- Stoy, P. C., El-Madany, T. S., Fisher, J. B., Gentine, P., Gerken, T., Good, S. P., Klosterhalfen, A., Liu, S., Miralles, D. G., Perez-Priego, O., Rigden, A. J., Skaggs, T. H., Wohlfahrt, G., Anderson, R. G., Coenders-Gerrits, A. M. J., Jung, M., Maes, W. H., Mammarella, I., Mauder, M., Migliavacca, M., Nelson, J. A., Poyatos, R., Reichstein, M., Scott, R. L., and Wolf, S.  
425 (2019). Reviews and syntheses: Turning the challenges of partitioning ecosystem evaporation and transpiration into opportunities, *Biogeosciences*, 16, 3747–3775, <https://doi.org/10.5194/bg-16-3747-2019>.
- Sun, W., Maseyk, K., Lett, C., & Seibt, U. (2016). Litter dominates surface fluxes of carbonyl sulfide in a Californian oak woodland. *Journal of Geophysical Research: Biogeosciences*, 121(2), 438-450.
- Sun, W., Kooijmans, L. M., Maseyk, K., Chen, H., Mammarella, I., Vesala, T., Levula, J., Keskinen, H. & Seibt, U. (2018).  
430 Soil fluxes of carbonyl sulfide (COS), carbon monoxide, and carbon dioxide in a boreal forest in southern Finland. *Atmospheric Chemistry and Physics*, 18(2), 1363-1378.
- Suni, T., Berninger, F., Vesala, T., Markkanen, T., Hari, P., Mäkelä, A., Ilvesniemi, H., Hänninen, H., Nikinmaa, E., Huttula, T., Laurila, T., Aurela, M., Grelle, A., Lindroth, A., Arneth, A., Shibistova, O. & Lloyd, J. (2003a). Air temperature triggers the recovery of evergreen boreal forest photosynthesis in spring. *Global change biology*, 9(10), 1410-1426.
- 435 Suni, T., Berninger, F., Markkanen, T., Keronen, P., Rannik, Ü. and Vesala, T. (2003b). Interannual variability and timing of growing-season CO<sub>2</sub> exchange in a boreal forest. *J. Geophys. Res.: Atmospheres*, 108(D9).
- Torrence, C. & Gilbert, P. (1998). A Practical Guide to Wavelet Analysis. *Bulletin of the American Meteorological Society*, 79(1), 61-78.
- Wehr, R., Commane, R., Munger, J. W., McManus, J. B., Nelson, D. D., Zahniser, M. S., Saleska, S. R. & Wofsy, S. C.  
440 (2017). Dynamics of canopy stomatal conductance, transpiration, and evaporation in a temperate deciduous forest, validated by carbonyl sulfide uptake. *Biogeosciences*, 14(2), 389-401.



- Whelan, M. E., Lennartz, S. T., Gimeno, T. E., Wehr, R., Wohlfahrt, G., Wang, Y., Kooijmans, L. M. J., Hilton, T. W., Belviso, S., Peylin, P., Commane, R., Sun, W., Chen, H., Kuai, L., Mammarella, I., Maseyk, K., Berkelhammer, M., Li, K.-F., Yakir, D., Zumkehr, A., Katayama, Y., Ogée, J., Spielmann, F. M., Kitz, F., Rastogi, B., Kesselmeier, J., Marshall, J.,  
445 Erkkilä, K.-M., Wingate, L., Meredith, L. K., He, W., Bunk, R., Launois, T., Vesala, T., Schmidt, J. A., Fichot, C. G., Seibt, U., Saleska, S., Saltzman, E. S., Montzka, S. A., Berry, J. A. and Campbell, J. E. (2018). Reviews and syntheses: Carbonyl sulfide as a multi-scale tracer for carbon and water cycles. *Biogeosciences*, 15(12), 3625-3657.
- Wohlfahrt, G., Brilli, F., Hörtnagl, L., Xu, X., Bingemer, H., Hansel, A., & Loreto, F. (2012). Carbonyl sulfide (COS) as a  
450 tracer for canopy photosynthesis, transpiration and stomatal conductance: potential and limitations. *Plant, cell & environment*, 35(4), 657-667.
- Wohlfahrt, G., Gerdel, K., Migliavacca, M., Rotenberg, E., Tatarinov, F., Müller, J., Hammerle, A., Julitta, T., Spielmann, F. M. & Yakir, D. (2018). Sun-induced fluorescence and gross primary productivity during a heat wave. *Scientific reports*, 8(1), 14169.
- Yang, F., Qubaja, R., Tatarinov, F., Rotenberg, E., & Yakir, D. (2018). Assessing canopy performance using carbonyl  
455 sulfide measurements. *Global change biology*, 24(8), 3486-3498.